

Interior pathways of the North Atlantic meridional overturning circulation

Amy S. Bower¹, M. Susan Lozier², Stefan F. Gary² & Claus W. Böning³

To understand how our global climate will change in response to natural and anthropogenic forcing, it is essential to determine how quickly and by what pathways climate change signals are transported throughout the global ocean, a vast reservoir for heat and carbon dioxide. Labrador Sea Water (LSW), formed by open ocean convection in the subpolar North Atlantic, is a particularly sensitive indicator of climate change on interannual to decadal timescales^{1–3}. Hydrographic observations made anywhere along the western boundary of the North Atlantic reveal a core of LSW at intermediate depths advected southward within the Deep Western Boundary Current (DWBC)^{4–9}. These observations have led to the widely held view that the DWBC is the dominant pathway for the export of LSW from its formation site in the northern North Atlantic towards the Equator^{10,11}. Here we show that most of the recently ventilated LSW entering the subtropics follows interior, not DWBC, pathways. The interior pathways are revealed by trajectories of subsurface RAFOS floats released during the period 2003–2005 that recorded once-daily temperature, pressure and acoustically determined position for two years, and by model-simulated ‘e-floats’ released in the subpolar DWBC. The evidence points to a few specific locations around the Grand Banks where LSW is most often injected into the interior. These results have implications for deep ocean ventilation and suggest that the interior subtropical gyre should not be ignored when considering the Atlantic meridional overturning circulation.

Profiling floats¹² released in the Labrador Sea during the 1990s showed little evidence of southward export of LSW in the DWBC^{13–16}. This result was surprising because the DWBC is widely thought to be the dominant LSW export pathway towards the subtropics and tropics. Why did these floats not follow the DWBC into the subtropics? Were they biased by upper-ocean currents when they periodically ascended to the sea surface to fix their position, as recently suggested by numerical model results¹⁷? Were they released mainly in the recirculating waters of the subpolar gyre? Or is the DWBC in fact not the dominant export pathway for LSW?

To address these questions, 76 acoustically tracked Range and Fixing of Sound (RAFOS) floats¹⁸, which do not need to surface to fix their position, were sequentially released in the DWBC near 50° N from 2003 to 2006 at two LSW depths, 700 and 1,500 m, for two-year drifting missions (see Fig. 1a and Methods for more details). Here we describe the spreading pathways of LSW revealed by the first 40 high-resolution RAFOS float trajectories, ten additional float displacement vectors and simulated trajectories (e-floats) from a high-resolution numerical ocean circulation model¹⁹.

All RAFOS floats initially drifted southward in the DWBC after release at 50° N (Fig. 1b). But a large fraction of the floats—about 75% (29/40)—escaped from the DWBC before reaching the southern tip or ‘Tail’ of the Grand Banks (43° N) (Fig. 2a and b) and drifted into the interior. Many of these followed an eastward path along the

subpolar–subtropical gyre boundary (Fig. 1a and b). Only 8% of all floats (3/40) followed the DWBC continuously from launch around the Tail of the Grand Banks. This is more than the number of profiling floats from the Labrador Sea that rounded the Tail of the Grand Banks in the DWBC (zero)¹⁴, but is still a remarkably low number in light of the expectation that the DWBC is the dominant southward pathway for LSW.

A larger percentage of the RAFOS floats—about 23% (9/40)—reached the subtropics via an interior pathway, indicated by the cluster of trajectories extending south of 42° N in the longitude band 40°–60° W (Fig. 1b). The warmer temperatures measured by these floats indicate that they crossed the Gulf Stream into the subtropical gyre. The dominance of the interior versus DWBC pathway is further supported by the larger ensemble of 50 RAFOS float displacement vectors (Fig. 1b inset)—about 24% (12/50) surfaced south of 42° N in the interior (east of 60° W). Furthermore, the largest southward float displacements over two years were made by floats following an interior, not DWBC path (Fig. 1b inset). Interior pathways for the southward spreading of LSW into the subtropics have been suggested previously^{7,9,17,20,21} but these float tracks offer the first evidence of the relative dominance of this pathway compared to the DWBC.

The RAFOS float trajectories reveal two primary locations where LSW escapes from the DWBC and enters the interior ocean—at the southeastern corner of Flemish Cap (especially for 1,500 m floats) and just upstream of the Tail of the Grand Banks (Fig. 2a and b). At these locations, the North Atlantic Current (Fig. 1a) is closest to the continental slope, supporting a previous conjecture that onshore excursions of the North Atlantic Current temporarily interrupt the flow of the DWBC and divert LSW into the interior¹⁵.

To complement this analysis of the necessarily limited number of RAFOS float trajectories, simulated trajectories were generated using the eddy-resolving (~1/12°) primitive equation Family of Linked Atlantic Models Experiment (FLAME) model¹⁹ (see Methods for details of trajectory computation). The e-float trajectories were calculated using the three-dimensional (x, y, z), time-varying model velocity fields to simulate fluid parcel motion as accurately as possible. The constant-pressure RAFOS floats drift only with the two-dimensional (x – y) flow field, but no significant differences were found in the model results using the two-dimensional or three-dimensional model velocity fields, in contrast to a previous modelling analysis of LSW pathways which used time-mean (as opposed to the time-varying fields used here) model velocity fields¹⁷ (see Supplementary Information).

Seventy-two e-floats were initialized in the DWBC near 50° N with the same spatial and temporal pattern as the RAFOS floats. The spread of the model and RAFOS float trajectories after two years is very similar (Fig. 3a). There is little evidence for a continuous DWBC pathway; rather, e-floats tend to recirculate within the subpolar gyre and drift southward into the subtropical gyre interior. The loss of

¹Department of Physical Oceanography, Woods Hole Oceanographic Institution, Woods Hole, Massachusetts 02540, USA. ²Division of Earth and Ocean Sciences, Nicholas School of the Environment, Duke University, Durham, North Carolina 27708, USA. ³IFM-GEOMAR Leibniz-Institut für Meereswissenschaften, Kiel, 24105, Germany.

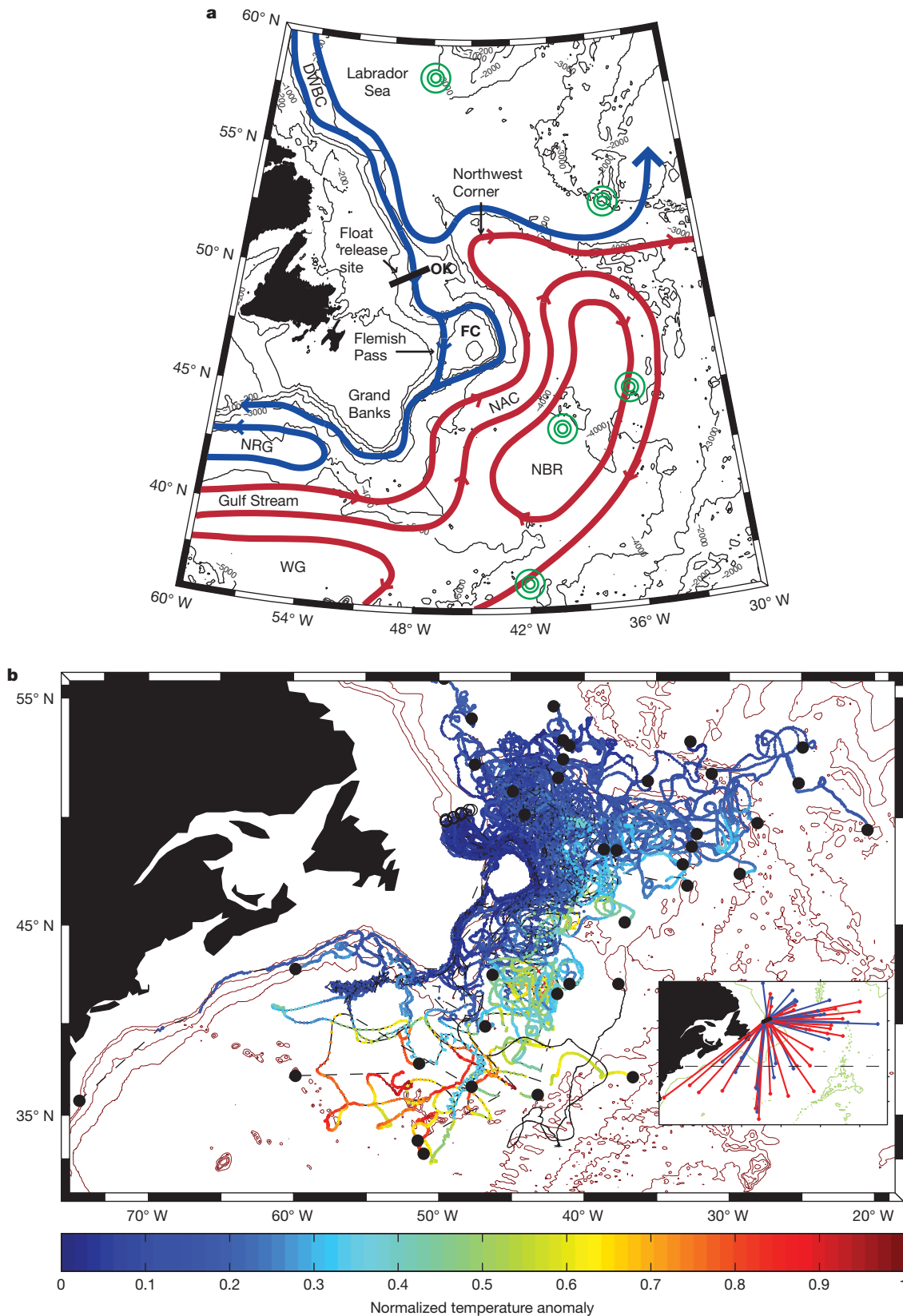


Figure 1 | Study area and RAFOS float trajectories at the LSW level in the western North Atlantic. **a**, Schematic diagram of the intermediate-depth circulation in the northwestern North Atlantic, with blue and red lines indicating cold and warm water pathways, respectively. Green concentric circles show locations of sound sources used to track floats. FC, Flemish Cap; NAC, North Atlantic Current; NBR, Newfoundland Basin Recirculation Gyre; NRG, Northern Recirculation Gyre; OK, Orphan Knoll; WG, Worthington Gyre. **b**, Two-year trajectories of 40 acoustically tracked

RAFOS floats released at 700 and 1,500 m in the DWBC near 50° N. Positions are indicated daily with colour-coded dots, where the colour indicates the normalized temperature anomaly, defined as $(T - T_i)/\delta T_{\max}$. T_i is each float's initial temperature, and δT_{\max} is the maximum temperature range observed by the floats as a group, 6.4 °C at 700 dbar and 1.8 °C at 1,500 dbar. Dashed lines indicate missing track. The inset shows the two-year displacement vectors for the same floats plus ten more that have yet to be processed, colour-coded by depth (red for 700 m and blue for 1,500 m).

e-floats from the DWBC is also very similar to that observed with the RAFOS floats (Fig. 2b).

This favourable comparison supports extending the integration to generate longer simulated trajectories (Fig. 3b and c), beyond the technical capabilities of the RAFOS floats. After five years, the Tail of the Grand Banks begins to stand out as a barrier to the westward spread of e-floats in the DWBC. Only after ten years is a thin collection of a small number of trajectories evident within the DWBC west

of the Grand Banks, emphasizing the importance of recirculation in the Newfoundland Basin in slowing the equatorward transport of recently ventilated LSW in the DWBC^{7,22}.

To quantify the Lagrangian spreading pathways of LSW, 7,280 e-floats were released and integrated for 15 years and a two-dimensional histogram of float position was mapped (Fig. 3d) (see Supplementary Information for details of map construction). The sharp drop in e-float concentration around the Grand Banks, and the southward penetration into the subtropical interior are clearly revealed. The e-floats are concentrated within an eddy-driven circulation that has previously been postulated to provide interior pathways from subpolar to subtropical latitudes^{20,21}.

A further demonstration of the lack of strong connectivity of LSW pathways around the Grand Banks is given by 15-year back trajectories for e-floats that arrived at Line W ($\sim 69^\circ$ W), where the properties and transport of the subtropical DWBC are being monitored (see <http://www.whoi.edu/science/PO/linew>) (Fig. 3e). Again, a strong discontinuity appears at the Tail of the Grand Banks. A thin ribbon of trajectories is traced from the Tail of the Grand Banks upstream to the western boundary of the Labrador Sea, but represents only a small fraction of the total at Line W. The model DWBC in the subtropical basin is mainly transporting waters that are recirculating north of the Gulf Stream and west of the Grand Banks in the Northern Recirculation Gyre (Fig. 1a)²³.

To quantify the relative importance of the DWBC versus interior pathways in the model, we mapped the transport associated with e-floats that drifted from the float release site at 50° N to 32° N within 15 years (Fig. 4; see Supplementary Information for details of map construction). We kept track of the e-floats that (1) never crossed offshore of the 4,000 m isobath into the interior (exclusively inshore), (2) were inshore of the 4,000 m isobath but may have crossed that isobath at some point (all inshore) and (3) were offshore of the 4,000 m isobath (all offshore). Transport values for each group as a function of distance along the boundary are tabulated in the Supplementary Information.

At the release site, all transport is inshore of the 4,000 m isobath. Moving southward along the path of the DWBC to the Tail of the Grand Banks, the all-inshore transport drops to about 62%, and the exclusively-inshore transport drops even more (43%). The transport located in the interior grows accordingly. A similar result for the all-inshore transport at the Tail of the Grand Banks was obtained in a previous modelling study¹⁷, from which the authors concluded that the DWBC was the dominant pathway for the export of LSW. However, as seen in Fig. 4, the all-inshore and especially the exclusively-inshore transports drop precipitously moving around the southern tip of the Grand Banks—at 55° W the all-inshore and exclusively-inshore transports are only 11.5% and 2.6%, respectively. At Cape Hatteras (36° N), only 3.1% of the transport being tracked is located inshore and 0.1% followed the DWBC continuously from the release site. South of 34° N, the interior transport begins to converge back towards the western boundary, but clearly the vast majority of the LSW transport tagged at 50° N in the DWBC that reached 32° N did so via an interior pathway. This result is consistent with the relatively larger number of RAFOS floats entering the subtropical gyre interior south of the Grand Banks (Fig. 1b) and with the observation of relatively young tracer ages there⁷.

The directions of LSW spreading presented here are generally consistent with those inferred from hydrographic and tracer studies: eastward and northward within the subpolar gyre, into the subtropical interior and along the DWBC^{4,7,9,24}. However, the new float observations and simulated float trajectories provide evidence that the southward interior pathway is more important for the transport of LSW through the subtropics than the DWBC, contrary to previous thinking. Though the DWBC is easier to observe—a well-defined, relatively stationary current close to shore compared to the vast, turbulent and unconstrained interior—our results suggest that further study of the interior subtropical gyre and the complex region around the Grand

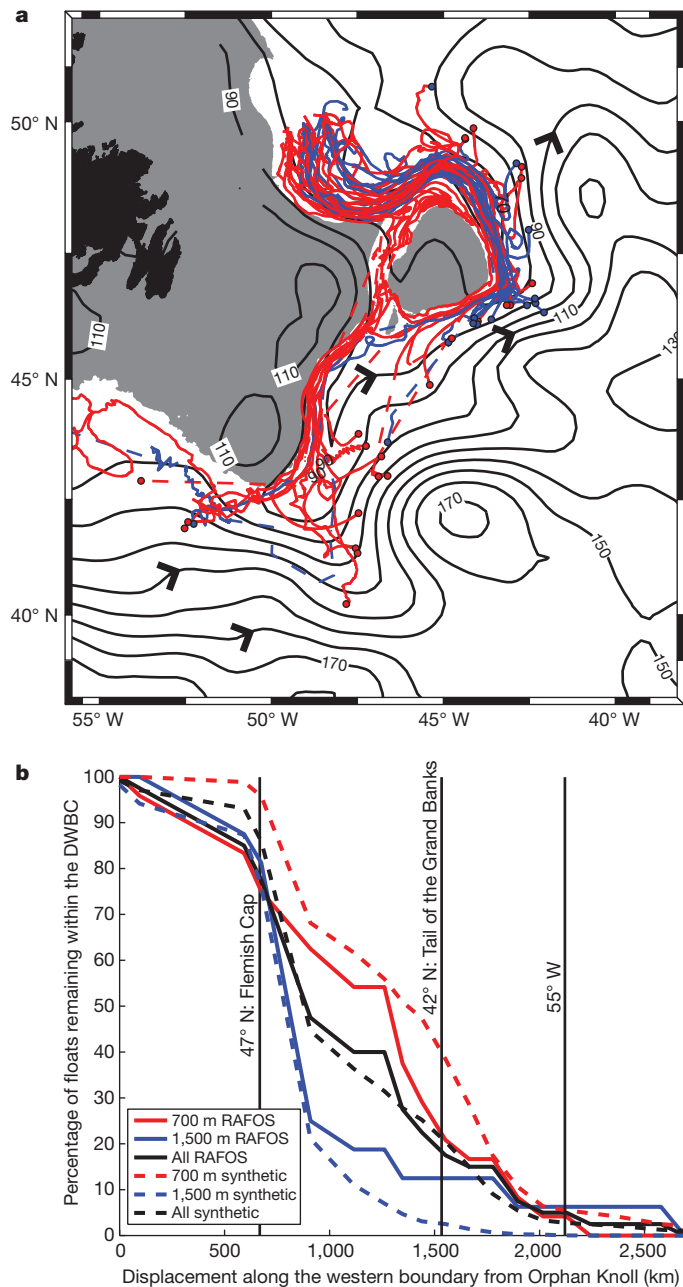


Figure 2 | Loss of floats from the DWBC. **a**, Trajectories of 40 RAFOS floats (blue, 1,500 m; red, 700 m) between launch position and the position where they first cross the 4,000 m isobath (coloured dots) illustrate where floats were most likely to leave the DWBC and drift into the interior. The mean path of the Gulf Stream and North Atlantic Current is shown with the mean absolute dynamic topography from Aviso (Archiving, Validation and Interpretation of Satellite Oceanographic data) for the float sampling time period. Arrows indicate direction of geostrophic surface flow, and the gradient is proportional to flow speed. The path of the North Atlantic Current is similar to that derived from subsurface floats²⁶ and hydrographic data²⁷. The 700-m isobath is shaded grey. **b**, Retention of RAFOS floats (solid lines) and e-floats (dashed lines) in the DWBC as a function of along-boundary distance from 50° N.

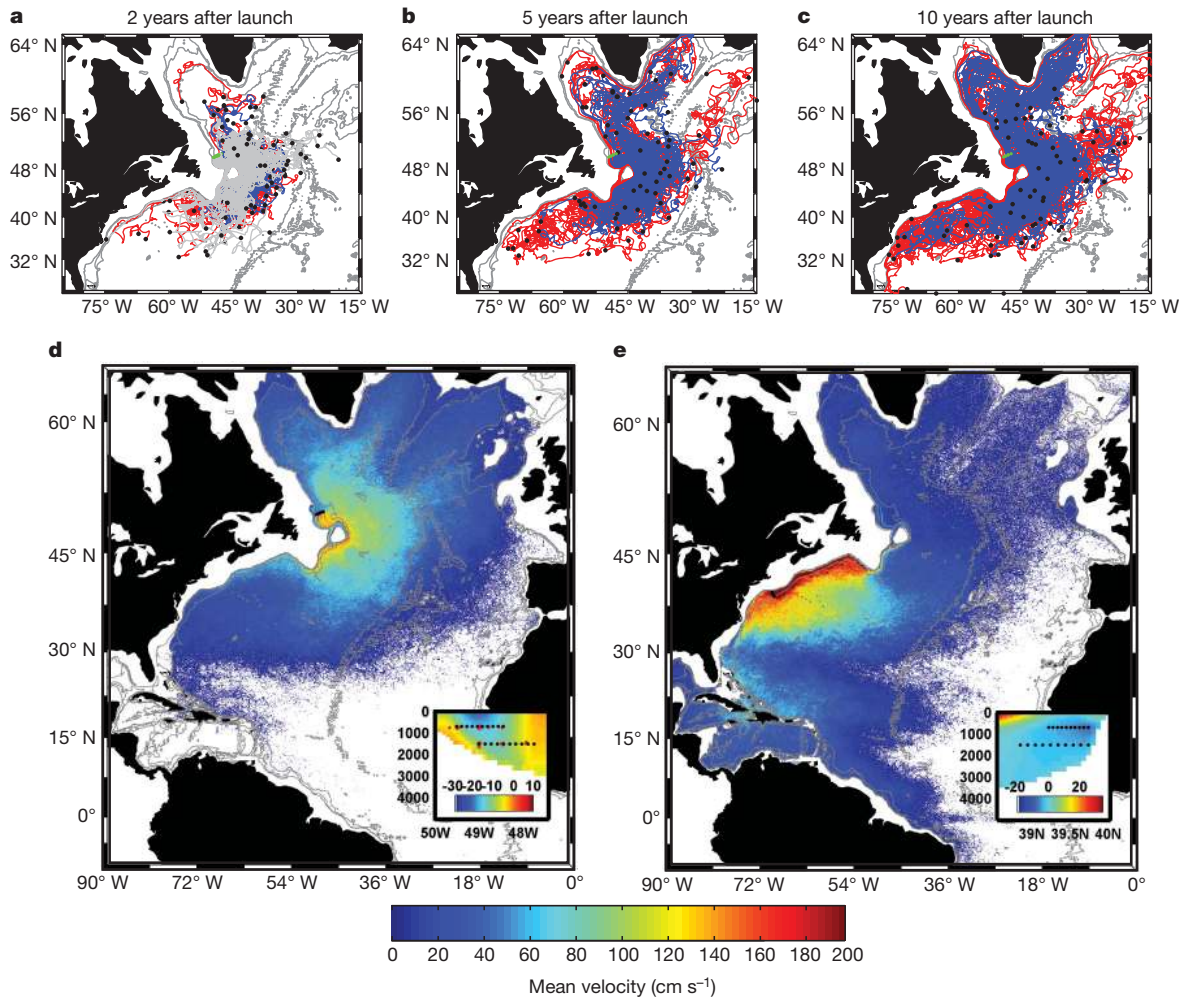


Figure 3 | Simulated trajectories from FLAME. Trajectories of (a) 2, (b) 5 and (c) 10 years for 72 e-floats at 700 m (red) and 1,500 m (blue), selected from an ensemble of 7,280 15-year trajectories initiated at the RAFOS float release sites near 50°N. The model trajectories were computed using the three-dimensional model velocity fields, so the virtual particles change their depth accordingly. The RAFOS trajectories (light grey) are shown in a for comparison. The endpoint of each e-float trajectory is marked with a black dot. Isobaths are shown in darker grey for 0, 700, 1,500 and 3,000 m. **d** and

e, 7,280 forward e-trajectories launched at Orphan Knoll (**d**) and 7280 backward trajectories launched at Line W (**e**) in the core of the DWBC, condensed into float location two-dimensional histogram maps. The float launch locations are shown in black. The insets to each map show the float launch locations at each site superposed on the mean velocity (in cm s^{-1}) cross-section from the FLAME model. The RAFOS and e-float launch points are shown with red and black dots, respectively.

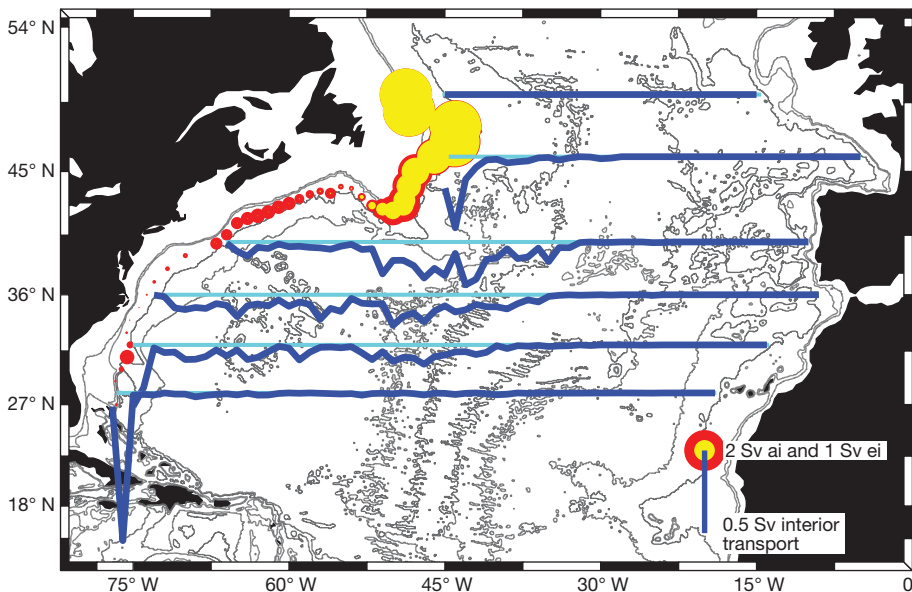


Figure 4 | Transport map for 1,338 e-floats released in the layer 703–1,548 m at 50° N that crossed the latitude 32° N within 15 years. Coloured circles indicate transport associated with all-inshore ('ai', red) and exclusively-inshore ('ei', yellow) e-floats, where circle radius is proportional to transport in Sv (see scale bar). Blue lines indicate transport associated with all-offshore ('ao') e-floats as a function of longitude for selected latitudes. Light blue lines show the zero reference for each blue line. Details on map construction as well as tabulated transport values are given in the Supplementary Information.

Banks is needed to understand better the pathways of the deep limb of the Atlantic Meridional Overturning Circulation.

METHODS SUMMARY

The RAFOS floats used in this study were released (nominally) in groups of six every three months between July 2003 and April 2005 along a section extending from Cape Bonavista, Newfoundland to Orphan Knoll. As the floats drifted, their positions were determined relative to sound sources moored in the eastern and western North Atlantic. The floats were isobaric (constant pressure) and ballasted to drift at two levels corresponding to the tracer cores of Upper LSW (700 dbar) and Classical LSW (1500 dbar). The floats internally recorded travel times from the sound sources, as well as temperature and pressure measurements once daily for two years, before returning to the surface and transmitting all the collected data via the Argos satellite-based data retrieval system.

The simulated trajectories presented in this study were generated using the FLAME model. This model was based on the MOM2.1 code²⁵ and modified as part of the FLAME project⁴. Following a ten-year spin-up from rest with climatological forcing, this model was run with interannually varying wind stresses and heat fluxes for the period 1987–2004. The model output consists of three-dimensional snapshots of horizontal velocity, temperature and salinity fields over the domain on a 1/12° resolution Mercator grid.

To calculate the simulated trajectories, model velocity fields from the years 1994, 1996 and 1998 were repeated sequentially for 15 years. These years represent a variety of forcing states as indicated by the North Atlantic Oscillation index. Model floats were initialized sequentially over the course of the first three years and every trajectory was computed for 15 years using 3-day snapshot, three-dimensional velocity fields. Thus the virtual floats are displaced both horizontally and vertically in accordance with the velocity fields to simulate water parcel movement as accurately as possible.

Full Methods and any associated references are available in the online version of the paper at www.nature.com/nature.

Received 24 April 2008; accepted 5 March 2009.

1. Lazier, J. Oceanographic conditions at ocean weather ship Bravo, 1964–1974. *Atmos. Ocean* **18**, 227–238 (1980).
2. Rhines, P. B. & Lazier, J. R. N. A 13-year record of convection and climate change in the deep Labrador Sea. In *Abstract Report of ACCP Principal Investigators Meeting* (NOAA Office of Global Programs, 1995).
3. Lazier, J., Yashayaev, I., Rhines, P., Hendry, R. & Clarke, A. Convection and restratification in the Labrador Sea, 1990–2000. *Deep-Sea Res. I* **49**, 1819–1835 (2002).
4. Talley, L. D. & McCartney, M. S. Distribution and circulation of Labrador Sea Water. *J. Phys. Oceanogr.* **12**, 1189–1205 (1982).
5. Molinari, R. L., Fine, R. A. & Johns, E. The Deep Western Boundary Current in the tropical North Atlantic Ocean. *Deep-Sea Res.* **39**, 1967–1984 (1992).
6. Pickart, R. S. Water mass components of the North Atlantic Deep Western Boundary Current. *Deep-Sea Res.* **39**, 1553–1572 (1992).
7. Smethie, W. M. Jr, Fine, R. A., Putzka, A. & Jones, E. P. Tracing the flow of North Atlantic Deep Water using chlorofluorocarbons. *J. Geophys. Res.* **105**, 14297–14324 (2000).
8. Stramma, L. *et al.* Deep water changes at the western boundary of the subpolar North Atlantic during 1996 to 2001. *Deep-Sea Res.* **1** **51**, 1033–1056 (2004).
9. Rhein, M. *et al.* Labrador Sea Water: pathways, CFC inventory, and formation rates. *J. Phys. Oceanogr.* **32**, 648–665 (2002).
10. Molinari, R. L. *et al.* The arrival of recently formed Labrador Sea Water in the Deep Western Boundary Current at 26.5° N. *Geophys. Res. Lett.* **25**, 2249–2252 (1998).
11. Bryden, H. L., Johns, W. E. & Saunders, P. M. Deep Western Boundary Current east of Abaco: Mean structure and transport. *J. Mar. Res.* **63**, 35–57 (2005).

12. Davis, R. E. The Autonomous Lagrangian Circulation Explorer (ALACE). *J. Atmos. Ocean. Technol.* **9**, 264–285 (1992).
13. Lavender, K. L., Davis, R. E. & Owens, W. B. Mid-depth recirculation observed in the interior Labrador and Irminger seas by direct velocity measurements. *Nature* **407**, 66–69 (2000).
14. Lavender, K. L., Owens, W. B. & Davis, R. E. The mid-depth circulation of the subpolar North Atlantic Ocean as measured by subsurface floats. *Deep Sea Res.* **1** **52**, 767–785 (2005).
15. Fischer, J. & Schott, F. A. Labrador Sea Water tracked by profiling floats—from the Boundary Current into the open North Atlantic. *J. Phys. Oceanogr.* **32**, 573–584 (2002).
16. Schott, F. A. & Brandt, P. in *Ocean Circulation: Mechanisms and Impacts* (eds Schmittner, A., Chiang, J. C. H. & Hemming, S.) 95 (American Geophysical Union, 2007).
17. Getzlaff, K., Boening, C. W. & Dengg, J. Lagrangian perspectives of deep water export from the subpolar North Atlantic. *Geophys. Res. Lett.* **33**, L21508, doi:10.1029/2006GL026470 (2006).
18. Rossby, H. T., Dorson, D. & Fontaine, J. The RAFOS system. *J. Atmos. Ocean. Technol.* **3**, 672–679 (1986).
19. Boening, C. W., Scheinert, M., Dengg, J., Biastoch, A. & Funk, A. Decadal variability of subpolar gyre transport and its reverberation in the North Atlantic overturning. *Geophys. Res. Lett.* **33**, L21501 (2006).
20. Lozier, M. S. Evidence for large-scale eddy-driven gyres in the North Atlantic. *Science* **277**, 361–364 (1997).
21. Lozier, M. S. The impact of mid-depth recirculations on the distribution of tracers in the North Atlantic. *Geophys. Res. Lett.* **26**, 219–222 (1999).
22. Schmitz, W. J. & McCartney, M. S. On the North Atlantic Circulation. *Rev. Geophys.* **31**, 29–49 (1993).
23. Hogg, N. G., Pickart, R. S., Hendry, R. M. & Smethie, W. J. Jr. The northern recirculation gyre of the Gulf Stream. *Deep-Sea Res.* **33**, 1139–1165 (1986).
24. Kieke, D. *et al.* Changes in the CFC inventories and formation rates of Upper Labrador Sea Water, 1997–2001. *J. Phys. Oceanogr.* **36**, 64–86 (2006).
25. Pacanowski, R. C. *MOM 2 (Version 2.0) Documentation User's Guide and Reference Manual*, Geophys. Fluid Dynam. Lab. Ocean Technol. Rep. 3.1 329 (GFDL/NOAA, 1996).
26. Rossby, H. T. The North Atlantic Current and surrounding waters: at the crossroads. *Rev. Geophys.* **34**, 463–481 (1996).
27. Kearns, E. J. & Rossby, H. T. Historical position of the North Atlantic Current. *J. Geophys. Res.* **C 103**, 15509–15524 (1998).

Supplementary Information is linked to the online version of the paper at www.nature.com/nature.

Acknowledgements We acknowledge the captains and crews of the R/V *Oceanus* and numerous Canadian fisheries research vessels, and scientists from the Northwest Atlantic Fisheries Centre in St. John's, Newfoundland, for their assistance in the deployment of the floats and sound sources used in this study. In particular, we thank E. Colbourne for his support of the float release programme. We also acknowledge J. Valdes and B. Guest for their expert technical support in the preparation of the floats, and H. Furey for providing float tracking. J. Fischer of IFM-GEOMAR provided several days of ship time to replace sound sources. We dedicate this work to the memory of F. Schott. The work was supported by the US National Science Foundation.

Author Contributions A.S.B. and M.S.L. contributed equally to this work. A.S.B. led the RAFOS float field programme, and analysed the float and altimetric data. M.S.L. led the modelling study and with S.F.G. analysed the simulated trajectories. C.W.B. provided the model output and assisted with the calculation of the simulated trajectories from FLAME.

Author Information Reprints and permissions information is available at www.nature.com/reprints. Correspondence and requests for materials should be addressed to A.S.B. (abower@whoi.edu) and M.S.L. (mslozier@duke.edu).

METHODS

RAFOS floats. The RAFOS floats used in this study were released (nominally) in groups of six floats every three months between July 2003 and April 2005 along a section extending from Cape Bonavista, Newfoundland to Orphan Knoll, in water depths between 1,400 and 2,800 m (see Supplementary Table S1 for details). As the floats drifted, their positions were determined relative to sound sources moored in the eastern and western North Atlantic. All but the first float setting were made from various Canadian research vessels by the Northwest Atlantic Fisheries Centre in St. John's, Newfoundland, during spring, summer and autumn cruises. To release RAFOS floats during winter, six dual-release floats were deployed during each autumn cruise in addition to the six regular floats. The dual-release floats each had a heavy length of chain attached that initially anchored them to the sea floor, creating a 'float park'²⁸. These floats were programmed to release the anchor chain on the following February 15th, and then drift to their ballast depth to begin their two-year mission.

The RAFOS floats used in this study were isobaric and ballasted to drift at two levels, corresponding to Upper LSW (700 dbar) and Classical LSW (1,500 dbar). The floats collected position, temperature and pressure information once daily for two years, then returned to the surface to transmit all the collected data via Service ARGOS.

Satellite altimetry. In Fig. 2a, the path of the Gulf Stream and North Atlantic Current were determined using maps of absolute dynamic topography produced by Ssalto/Duacs at Collecte Localisation Satellites, a subsidiary of the French Space Agency (CNES) and the French Research Institute for Exploration of the Sea (IFREMER). This product is generated using all available satellite missions since 1992. With support from CNES it is distributed online by Aviso (http://www.jason.oceanobs.com/html/donnees/produits/hauteurs/global/madt_uk.html). The maps of absolute dynamic topography combine gridded ($1/3^\circ$) sea level anomaly fields with the Combined Mean Dynamic Topography (Rio05)²⁹.

Synthetic float trajectory calculations. The synthetic trajectories used in this study were generated using the FLAME model, which was based on the MOM2.1 code and modified as part of the FLAME project¹⁹. Following a ten-year spin-up from rest with climatological forcing, this model was run with interannually varying wind stresses and heat fluxes for the period 1987–2004. Model output consists of three-dimensional snapshots of horizontal velocity, temperature and salinity fields over the domain on a $1/12^\circ$ resolution Mercator grid. In the vertical, the domain was split into 45 z -coordinate levels. The vertical velocity was computed from the horizontal velocity by requiring that the local divergence of the three-dimensional velocity field be zero throughout the model domain.

Velocity fields from FLAME model years 1994, 1996 and 1998, repeated sequentially, were used for the 15-year trajectories. These years represent a variety of forcing states as indicated by the North Atlantic Oscillation index. The e-floats were released sequentially over the course of the first three years and every trajectory was computed for 15 years using 3-day snapshot three-dimensional model velocity fields. We note that throughout the study, '700 m' and '1,500 m' e-floats refer to their approximate depths of float initialization. Subsequent e-float

positions are estimated from the three-dimensional model velocity fields, so the virtual floats are displaced both horizontally and vertically to simulate water parcel movement as accurately as possible.

Computation of float loss from the DWBC. See Fig. 2b. Because the DWBC generally flows inshore of the 4,000 m isobath in the study region, a RAFOS or e-float was considered out of the boundary current if it crossed this isobath into deeper water. To determine the number of floats that remain within the DWBC at different points along the coast, ten boxes, each spanning the width of the continental slope, were defined along the boundary. The number of floats that passed through each box was counted. In this analysis, floats that left the DWBC at any point along the boundary were never counted again, even if they happened to re-enter one of the boxes. Thus, the number of floats remaining within the DWBC includes only those floats that have remained in the DWBC continuously since launch (also called exclusively-inshore floats).

Construction of e-float position histograms. See Fig. 3d and e. To present the Lagrangian pathway information from the thousands of synthetic trajectories used in this study efficiently, a two-dimensional histogram of float positions, essentially a map of float concentration, was used. A count was made of the number of floats that passed through each $1/12^\circ$ horizontal bin; repetitions of the same float were counted. The units on the two-dimensional histogram are the number of floats passing through each bin. Histograms of the 700 and 1,500 m subsets of the float population are qualitatively similar to the whole population histograms.

Construction of transport map. See Fig. 4. The e-floats were initialized at the RAFOS float release site (near 50° N) in the layer spanning 703 to 1,540 m. The e-floats were launched on a 7-level grid with nodes at: 744, 828, 920, 1,022, 1,140, 1,280 and 1,448 m. Each e-float was assigned a transport computed from the velocity, layer thickness and cell width at the e-float's release location. The layer thicknesses used to compute the transport tag for each float range from 78–184 m, increasing with increasing layer depth. The three-dimensional trajectories were computed using the repeating cycle of 1994, 1996 and 1998 3-day updated velocity fields for 15-year integrations. At release, the total transport was 12 Sv in the layer (for each of the 36 launch dates) divided between a grand total of 6,539 floats. Floats were launched every 30 days for the first three years (and because the velocity field repeated itself after the first three years, no new initializations were made after that point). Only those e-floats that crossed 32° N within 15 years were retained, which accounts for the movement of 2 Sv (average transport per launch initialization) among a total of 1,338 e-floats. Longer integrations gave very similar results.

28. Zenk, W., Pinck, A., Becker, S. & Tillier, P. The Float Park: A new tool for a cost-effective collection of Lagrangian time series with dual release RAFOS floats. *J. Atmos. Ocean. Technol.* **17**, 1439–1443 (2000).
29. Rio, M., Schaeffer, P., Lemoine, J. & Hernandez, F. Estimation of the ocean Mean Dynamic Topography through the combination of altimetric data, in-situ measurements and GRACE geoid: from global to regional studies. In *Proc. of the GOCINA Int. Workshop* (GOCINA, 2005).